Iranian Journal of Materials Forming 13 (1) (2026) 30-44

Online ISSN: 2383-0042

IJMF

Iranian Journal of Materials Forming

Journal Homepage: http://ijmf.shirazu.ac.ir

Research Article

Feasibility of Deep Crack Repair Using a Novel Friction Stir Chip Welding Process

Ali Bazrafshan Tanha[1], Seyed Mohammad Hossein Seyedkashi[1*], Moosa Sajed[2] and Habibollah Rastegari[3]

[1] Department of Mechanical Engineering, University of Birjand, Birjand, Iran
[2] Department of Mechanical Engineering, Azarbaijan Shahid Madani University, Tabriz, Iran
[3] Department of Mechanical and Materials Engineering, Birjand University of Technology, Birjand, Iran

ARTICLE INFO

Article history:

Received: 24 September 2025
Reviewed: 14 October 2025
Revised: 27 October 2025
Accepted: 31 October 2025

Keywords:

Friction stir chip welding
Recycling
Aluminum 7075
Machining chips
Crack repair

Please cite this article as:

Bazrafshan Tanha, A., Seyedkashi, S. M. H., Sajed, M. & Rastegari, H. (2026). Feasibility of deep crack repair using a novel friction stir chip welding process. *Iranian Journal of Materials Forming*, *13*(1), 30-44. https://doi.org/10.22099/IJMF.2025.54371.1351

ABSTRACT

A new friction stir chip welding (FSCW) method is presented to use waste machining chips for repairing deep cracks. This technique provides an economical solution for industry by reducing landfill waste and minimizing the energy-intensive demand for primary aluminum production. Aluminum 7075 was used to evaluate the feasibility of this method. The crack was removed by an in-depth hole and filled with machining chips, which were subsequently welded using non-consumable tools. The most effective parameter for achieving a proper joint was the input heat, governed by the tool rotational speed and holding time. The effects of these parameters on weld quality, microstructure and hardness across different welding zones were investigated. The results showed that increasing the tool rotational speed and holding time led to higher heat input. The specimen welded at the highest speed and holding time exhibited the greatest hardness and strength. Specimens with a continuous structure demonstrated higher hardness, and vice versa.

1. Introduction

Welding processes can be divided into two categories: fusion welding and solid-state welding. In the solid-state welding method, no melting takes place. In this method, applying a compressive force causes plasticization and deformation at the contact surface of the components, causing the two parts to join together. Friction stir welding (FSW) is a relatively new solid-state welding method, which is an environmentally friendly technology for joining metallic parts that produces high-quality welds for low-density ductile metals such as aluminum, magnesium, titanium, and their alloys [1].

* Corresponding author
E-mail address: seyedkashi@birjand.ac.ir (S. M. H. Seyedkashi)
https://doi.org/10.22099/IJMF.2025.54371.1351

This method has a wide range of applications and advantages, such as no need for consumables and desirable mechanical properties. In the FSW process, a non-consumable rotating tool with a specific geometry is used. The combined rotational and linear movement of the tool inside of welded parts creates high friction and heat causing them to be joined together [2].

In this process, defects such as porosity, crack formation, oxidation and other imperfections that occur during the fusion welding are less common. For this reason, this method has become the most popular choice for welding lightweight boats, car bodies, fuel tanks, aircraft wing structures and electronic, and circuit devices. The main parameters of friction stir welding consist of tool rotational speed, tool angle, tool geometry, tool force on the workpiece and tool linear speed. These parameters affect the flow of material and heat distribution at the joint. The microstructure and mechanical properties of the resulting weld are affected by how the mentioned parameters are used.

Friction stir spot welding (FSSW) is another type of FSW. In this process, the tool penetrates just vertically into the part and creates the connection at a single point. The most important parameters in this process are tool rotational speed, depth and holding time. Changes in the above parameters cause variations in the mechanical and microstructural properties of the weld [3, 4]. Fig. 1(a-c) shows the main stages of the FSSW process. This process can be divided into three main stages: plunging, dwelling and retracting. During the plunging stage (Fig. 1(a)), the rotating pin of the tool plunges into the workpiece, generating heat through friction. At the end of penetration, the tool keeps rotating for a certain period of time to create stirring (Fig. 1(b)) and then the rotating tool is retracted from the material, leaving a keyhole (Fig. 1(c)), which is the main disadvantage of the FSSW. Two-stage friction stir spot welding (TFSSW) is a backfilling process which was developed to fill the keyhole and improve the joint strength of the FSSW process in two steps [5]. The first step consists of the conventional FSSW process, as shown in Fig. 1(a-c), while the second step involves filling the keyhole with a plug, as shown in Fig. 1(d-f). In the second step, a pinless tool is plunged into the keyhole filled with a plug (Fig. 1(d)). This action aims to close the keyhole and consolidate the weld. Then, it dwells in the material for a short period (Fig. 1(e)). This maintains the forging pressure and heat, allowing for further material consolidation and grain refinement, effectively closing any remaining keyhole or voids. Finally, the pinless tool is retracted from the material, leaving a flat, consolidated spot weld with no keyhole (Fig. 1(f)).

Sharma et al. [6] investigated the FSW of 2000 series aluminum alloy at seven different combinations of tool rotational speed and feed rate. The metallurgical behavior of the weld joints was analyzed using optical microscopy. It was observed that microhardness and corrosion resistance were enhanced at lower rotational speeds coupled with higher feed rates. Malopheyev et al. [7] investigated the FSW of 6061 aluminum sheets. Using microhardness testing, it was observed that the hardness of the specimens in the weld zone was less than that of the base metal. Ahmed et al. [8] conducted FSSW on AA6082-T6 aluminum alloy. The welding process was performed at a constant holding time of 3 seconds and at different rotational speeds of 400, 600, 800 and 1000 rpm. The results showed that although joints were successfully formed at all four rotational speeds, the specimen with a rotational speed of 600 rpm exhibited the highest hardness among the produced joints. Fereiduni et al. [9] studied the FSSW of steels and aluminum alloys. Their results showed that increasing the holding time caused a decrease in joint strength, while increasing the tool rotational speed led to an increase in strength. Yuan et al. [10] employed the FSW refilling method to repair the residual hole defects formed at the end of the FSW process in AA7475 aluminum alloy plates. They investigated the macroscopic defects and mechanical properties of the repaired joints. The results showed that the exit hole was successfully refilled after the process. Li et al. [11] performed refill FSSW on 2A12-T4 aluminum alloy and investigated the effects of tool rotational speed on weld formation, microstructure evolution and mechanical properties. The microstructure of the joints revealed variations in grain size and sediment distribution across

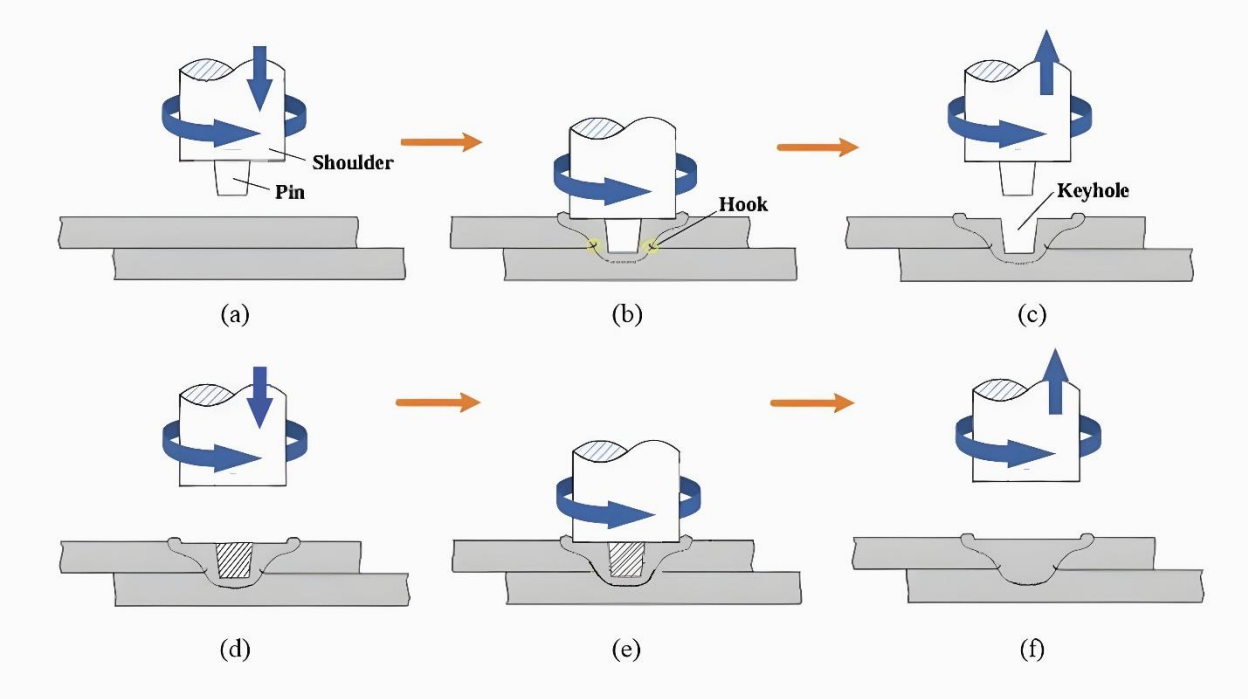

Fig. 1. Schematic of the two-stage friction stir spot welding (TFSSW) process: (a) pin tool plunging, (b) pin tool dwelling, (c) retracting, (d) pinless tool plunging, (e) pinless tool dwelling, (f) retracting.

the width direction. As the tool rotational speed increased from 900 to 1300 rpm, the hardness of the backfill zone decreased. Sajed [12] conducted a study on two-stage FSW of AA1100 aluminum alloy to achieve a void-free weld. This process was performed using two conventional welding tools and a backfilling step conducted in two steps. The tool rotational speed and backfilling tool shoulder diameter were found to have the greatest effect on weld strength, whereas the holding time had no significant effect on joint strength. Using a filler tool with a larger shoulder diameter and a lower rotational speed resulted in a stronger bond. Sajed and Seyedkashi [13] presented a new method for repairing deep cracks in aluminum plates. In this method, called multi-layer friction stir plug welding, a hole with a specific geometry was first created at the crack location. Welding was then performed using several plugs made from the parent material and a set of non-consumable rotating tools. The plugs were welded to each other and to the hole wall. The tool rotational speed and holding time were the main parameters investigated during this process. The results showed that a higher tool rotational speed and a shorter holding time resulted in a stronger bond.

Nowadays, new solid-state recycling processes, such as severe plastic deformation techniques like equal-channel angular pressing (ECAP) and friction stir consolidation (FSC), are being developed to directly convert aluminum chips into bulk, reusable forms. Shigematsu et al. [14] studied the FSW of recycled A6061 aluminum plates, which were fabricated by hot extrusion of machined chips, and analyzed the mechanical and structural properties of the resulting welds. They investigated the hardness distribution and microstructural changes in the friction stir zone and base metal, and examined the effects of post-welding heat treatment on the joined specimens. Haase et al. [15] studied the direct conversion of AA6060 aluminum alloy machining chips into finished products through hot extrusion followed by cold extrusion, focusing on the effectiveness of different extrusion dies. Li et al. [16] studied the FSC of AA6061 aluminum machining chips to produce solid discs, analyzing the process progression through tool motion, consolidation force, power history, and macro/microstructure observations. They also conducted a design of experiments to quantify the effects of die rotational speed, compressive force, and processing time on the consolidated material volume,

and employed a numerical model to predict density and temperature evolution. El-Mehtedi et al. [17] investigated the solid-state recycling of pure aluminum AA1090 machining chips using the friction stir extrusion (FSE) process. They conducted a finite element simulation to optimize the die design and process parameters, then experimentally extruded the chips and analyzed the resulting wire's microstructure and microhardness. Abbas et al. [18] studied the surface roughness of solid-state recycled 6061 aluminum alloy chips, which were processed through cold compaction, hot extrusion, and subsequent ECAP for up to three passes.

Yavari Nouri et al. [19] proposed a novel modified friction stir extrusion process for producing aluminum/steel double-layered wire using aluminum chips for the outer layer. They investigated the effects of tool rotational speed and feed rate on the adhesion strength and surface cracking behavior of the specimens. Laurent-Brocq et al. [20] investigated the solid-state recycling of AA6060 aluminum alloy chips, focusing on quantifying and localizing oxygen contamination throughout the process. Buffa et al. [21] developed an experimental and numerical study to enhance the industrial efficiency of recycling aluminum alloy chips into thin AA6082-T6 wires through the friction stir extrusion. Their study involved validating a numerical model for tool design optimization and systematically analyzing the effects of tool rotation and force on the mechanical properties and energy consumption of the produced wires. Carta et al. [22] investigated the viability of an innovative solid-state recycling method for AA6063 aluminum alloy chips through direct hot rolling, which involved compacting, heat-treating, and then hot-rolling the chips, with a bulk material used as a comparative control. Bhardwaj et al. [23] used aluminum chips to refill the pinhole generated in the friction stir process. They studied rotational speed, plunge depth during welding, and plunge depth during refilling on maximizing the load-bearing capacity of the joint. Several review papers have also summarized the literature on various processes used for re-using machining chips [24-26].

The evolution of friction stir welding (FSW) has witnessed significant innovations in process variants designed to overcome inherent limitations. For instance, Han et al. [27] introduced a probeless friction spot extrusion technique to eliminate the keyhole defect, a common weakness in traditional spot welds. Their research demonstrated that joining could be successfully achieved through a combination of mechanical interlocking and solid-state diffusion, with the tool shoulder design playing a critical role in influencing material flow and determining joint strength. Similarly, Heidarzadeh et al. [28] explored submerged FSW to mitigate the problematic loss of hardness in the thermo-mechanically affected zone (TMAZ) of dissimilar aluminum joints. By employing a water medium to control heat input, they achieved a remarkable improvement, reducing hardness loss in the TMAZ to only 13%, compared to the 57% typically reported in conventional FSW processes. They also observed a grain subdivision phenomenon in the AA6061 side of the joint, a restoration mechanism rarely reported in previous studies. They further attributed the finer grain structure in the AA7075 stir zone (SZ) to variations in precipitate morphology and size, which influence recrystallization behavior. This emphasis on microstructural evolution is crucial for explaining the mechanical properties measured in these joints, creating a direct link between processing parameters, metallurgical transformations, and the final performance. Panda et al. [29] employed a Genetic Programming (GP) approach to model the FSW process, generating highly accurate functional expressions for tensile properties and identifying tool rotational speed as the most dominant parameter. This data-driven methodology provides an effective tool for determining optimal parameter sets, such as a rotational speed of 1050 rpm and an axial force of 8 kN for high strength.

Table 1. details and compares six prominent solid-state techniques derived from the foundational friction stir welding process. It systematically outlines each method's primary objective, ranging from joining and spot welding to recycling scrap into new products and engineering surface composites. The comparison

Table 1. Comparison of solid-state processes for aluminum alloys

Method	Primary objective	Tool design	Ability to integrate recycled material	Key features	Applications
Conventional FSW	Join plates in butt, lap, or T-joint configurations.	Rotating shoulder + pin (cylindrical, conical polygonal, threaded, tapered).	No	Continuous welds; grain refinement in stir zone (SZ); Widely used in aerospace and automotive.	Aerospace structures, automotive components, marine applications.
FSSW	Create spot welds in lap joints.	Rotating tool plunged to set depth; may have threads, flats, or special profiles.	No	Spot joining capability.	Automotive spot joints, electronic enclosures, patch repairs.
Friction stir extrusion (FSE)	Recycle metal scraps (chips, powder) directly into wires, rods, or tubes.	Rotating die with extrusion channel; die shoulder often with scroll features or tapered angles. Common tool material: H13 steel.	Yes - Directly uses machining chips or powder as feedstock.	Single-step process; avoids remelting; no material oxidation losses; induces severe plastic deformation (SPD) for grain refinement; can produce metal-matrix composites (MMCs). Can be continuous (CFSE).	Wire production from scrap; in-house recycling of machining chips; tube manufacturing; composite wires/tubes (e.g., Al/SiC).
Friction stir consolidation (FSC)	Consolidate machining chips into fully dense disks or billets.	Similar to FSE but designed for consolidation rather than extrusion.	Yes - Directly uses machining chips.	Creates fully dense, solid components from scrap; Solid-state processing.	Disk/billet production from scrap; bulk material recycling.
Friction stir consolidation welding (FSCW)	Integrate recycled material into new joints or structures.	Custom tool for simultaneous consolidation and welding; designed to mix and consolidate recycled material.	Yes - Specifically designed for recycled material integration.	Novel approach combining consolidation and welding in one step; Enhanced sustainability.	Sustainable structural joints; repair with recycled material; green manufacturing.
Friction stir processing (FSP)	Modify surface layer microstructure; Produce surface composites by embedding reinforcing particles.	Non-consumable tool with shoulder and pin (similar to FSW). Variants: Pinless tool (for initial closure). DFSP tools with internal powder channels.	Yes - Can use recycled materials (e.g., fly ash) or industrial waste as reinforcement.	Solid-state surface engineering; induces grain refinement via dynamic recrystallization (DRX); eliminates casting defects; improves hardness wear, and corrosion resistance.	Surface hardening; wear-resistant coatings; corrosion-resistant layers bio-implant surfaces; automotive and aerospace components.

also highlights key aspects such as critical tool design characteristics, the crucial ability to integrate recycled material, and the distinctive features of each process. Furthermore, the table lists typical industrial applications across the aerospace, automotive, and sustainable manufacturing sectors [30-33].

In this paper, a modified two-stage FSSW process is proposed for repairing deep cracks in the workpiece. In this method, machining chips of the same material as the base metal are used as the filling material; therefore, the process is referred to as friction stir chip welding (FSCW). By employing this technique, deep defects of any height in various workpieces can be repaired. The main difference between this method and the multilayer friction stir plug welding process lies in the use of machining chips instead of plugs, which has a totally different mechanism with fewer processing stages. This technique not only returns the wasted chips to the consumption cycle but also aligns with the requirements of sustainable production. Moreover, the use of chips offers better adaptability to irregular crack geometries compared to preformed plugs.

2. Materials and Methods

Aluminum and its alloys hold a very prominent position in industrial applications, often ranking as the second most widely used metal globally after steel. Recycling of aluminum is important because it significantly reduces energy consumption, water pollution, and greenhouse gas emissions associated with primary aluminum production. In this study, AA7075 aluminum cubes were used. AA7075 aluminum alloy is used in transportation

industries such as aerospace, marine, and automotive due to its good mechanical properties, toughness, fatigue resistance, low density, and high strength-to-weight ratio. First, an aluminum billet with a height of 25 mm was cut using a band saw into 35 × 35 × 25 (mm^3) cubes. Then, the specimens were ground. After that, a 5 mm diameter hole with a depth of 8 mm and a 10 mm diameter hole with a depth of 3 mm was created in the center of the specimens. This stepped hole was filled with aluminum chips and manually compressed using a punch and hammer.

This process requires two tools: a pin-and-shoulder tool and a pinless tool. The tools used in this study were made of H13 steel, which is a hot-work tool steel with excellent wear resistance, suitable for applications requiring high hardness and resistance to elevated temperatures.

A milling machine was used to perform the FSCW process. Considering the geometry of the aluminum parts, their height was considered such that no special fixture was needed for performing FSCW. The parts were securely clamped using a bench vise, and the welding process was then performed. The hole in the workpiece was first filled with chips, which were manually pressed using a punch and hammer. The process was carried out in three stages. First, a pinless tool was rotated and moved vertically into the hole to a depth of 1 mm in order to generate heat (Fig. 2(a-b)). It was held in this position for 30 seconds. This stage was necessary to soften and form an initial bond between the chips, preventing them from spilling out of the hole. The importance of this pre-heating stage is substantiated by experimental findings from analogous solid-state processes, specifically multilayer friction stir plug welding (MFSPW) [13]. In that work, omission of a pinless tool for initial conditioning led to two specific failure modes directly relevant to the present process. The use of only conventional pinned tools resulted in elongated refilling defects and voids, attributed to unfavorable material flow pattern. These defects were eliminated only when a pinless tool was employed, a result that directly parallels the function of the pre-heating stage in this study. This stage effectively conditions the entire bonding area and prevents incomplete bonding and void formation at the interfaces. Therefore, the pre-heating stage serves as an essential thermal management strategy that prevents critical defects by ensuring proper initial material flow, mitigates interfacial cracking by avoiding thermal shock, and establishes a uniform thermal baseline for robust bonding.

In the second stage tool, the welding tool was used with a specified rotational speed and holding time. The pin was inserted into the workpiece to a depth of 3.5 mm and held for a certain time (Fig. 2(c-d)). Initially, the tool was inserted 2 mm into the workpiece until the tool shoulder contacted the upper step of the hole to generate additional heat. Then, it was moved another 1.5 mm into the workpiece. The chips in the hole were welded to each other and to the bottom and wall of the hole, completely filling it. When the tool was retracted from the workpiece, the space occupied by the pin remained hollow in the workpiece. To fill this void, the same pinless tool used in the first stage was employed again. The hollow space was refilled and pressed again with chips. The pinless tool was then moved 1.5 mm into the workpiece at a certain rotational speed and held for a certain time (Fig. 2(e)). Finally, the tool was retracted from the workpiece (Fig. 2(f)).

During the machining process, rotational speed, depth of cut, and feed rate are the parameters that most significantly influence chip geometry and dimensions. In the present study, aluminum machining chips produced under a tool rotational speed of 800 rpm, a depth of cut of 0.25 mm, and a feed rate of 12 mm/min were used. This combination was selected based on primary experiments to obtain chips with suitable dimensions for the designed experiments.

In this study, the objective was to determine the optimal combination of welding variables using the two-level factorial design of experiments (DOE) method. In the FSCW process, the tool rotational speed and holding time are the most important parameters that affect the mechanical and microstructural properties of the weld. Therefore, these two factors were selected as the effective parameters, each evaluated at two levels. The

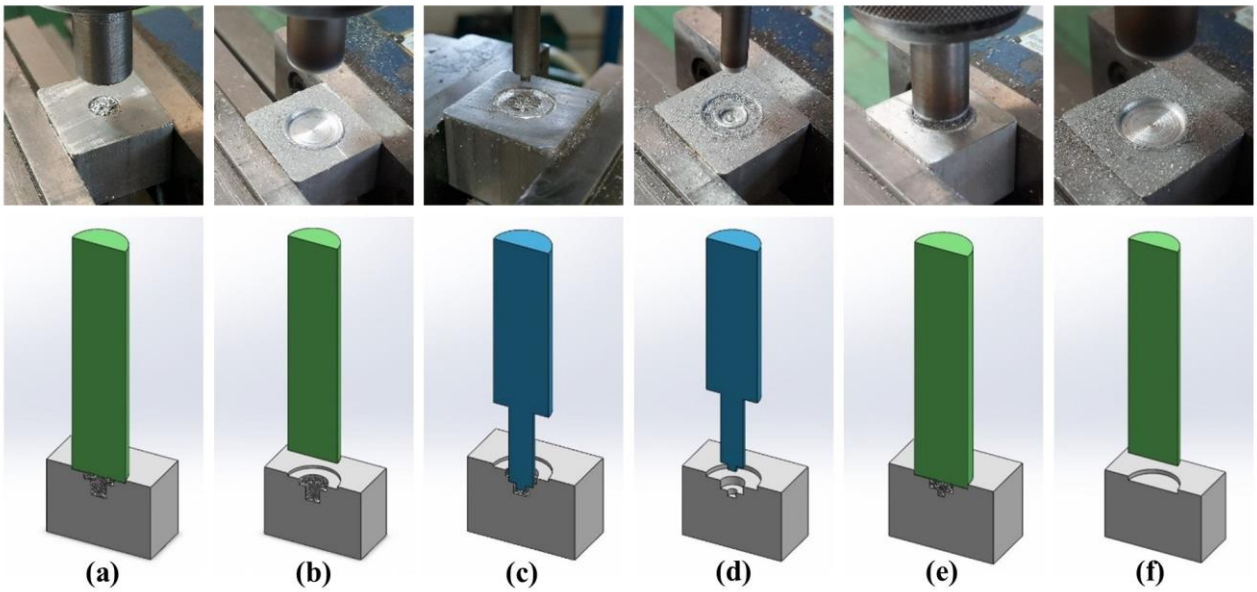

Fig. 2. Schematic of each experiment: (a) first stage, (b) retracting, (c) second stage (welding), (d) retracting, (e) third stage (refilling), (f) retracting.

experiments were thus performed according to the conditions summarized in Table 2.

Table 2. The FSCW process variables (DOE table)

No.	Stage 1 (welding) and Stage 2 (refilling)	
	rotational speed (rpm)	holding time (s)
#1	1250	10
#2	1250	20
#3	1600	10
#4	1600	20

In order to study the quality and microstructure of the weld cross-section, the specimens were cut from the middle of the weld area using a wire-cut machine. The samples were then sanded using 400~2500 grit sandpapers in accordance with the specimen preparation standard (ASTM E3). The parts were polished and then etched using an etchant containing 5 mL of HNO_3, 3 mL of HCL, 2 mL of HF and 90 mL of water for 30 seconds. The microstructures of the different weld areas were examined using an Olympus BH60 optical microscope. In addition, to determine the hardness values in the base metal and weld regions, the Rockwell method was used using a 60 kgf load at eight measurement points with a KOOPA-UV1 hardness tester.

3. Results and Discussion

All four specimens exhibited a uniform and relatively flawless joint in appearance, with the holes well filled. However, variations in the welding parameters resulted in differences in weld quality. To evaluate these differences, the microstructure images of the weld cross-section were analyzed and compared.

Fig. 3 shows the cross-section of the welded specimens produced under different parameters. As illustrated, the FSCW process using machining chips was effective in forming joints and filling the hole. The overall weld quality in this process depends on the successful consolidation of the machining chips and the formation of a strong metallurgical bond between the consolidated chips and the parent material. This behavior is primarily governed by heat input and material flow, both controlled by the tool rotational speed and holding time. Although the proper joints were obtained in all conditions, defects were observed near the bottom of the holes due to insufficient material flow and inadequate heat generation. The heat input, which depends on both the rotational speed and holding time, plays a critical role. Higher rotational speed and longer holding times generate greater heat, leading to better chip flow and their greater welding to each other and the hole wall. In specimen #1, both the holding time and tool rotational speed were at their lowest level (1250 rpm 10 s, respectively). As a result, sufficient heat and mechanical

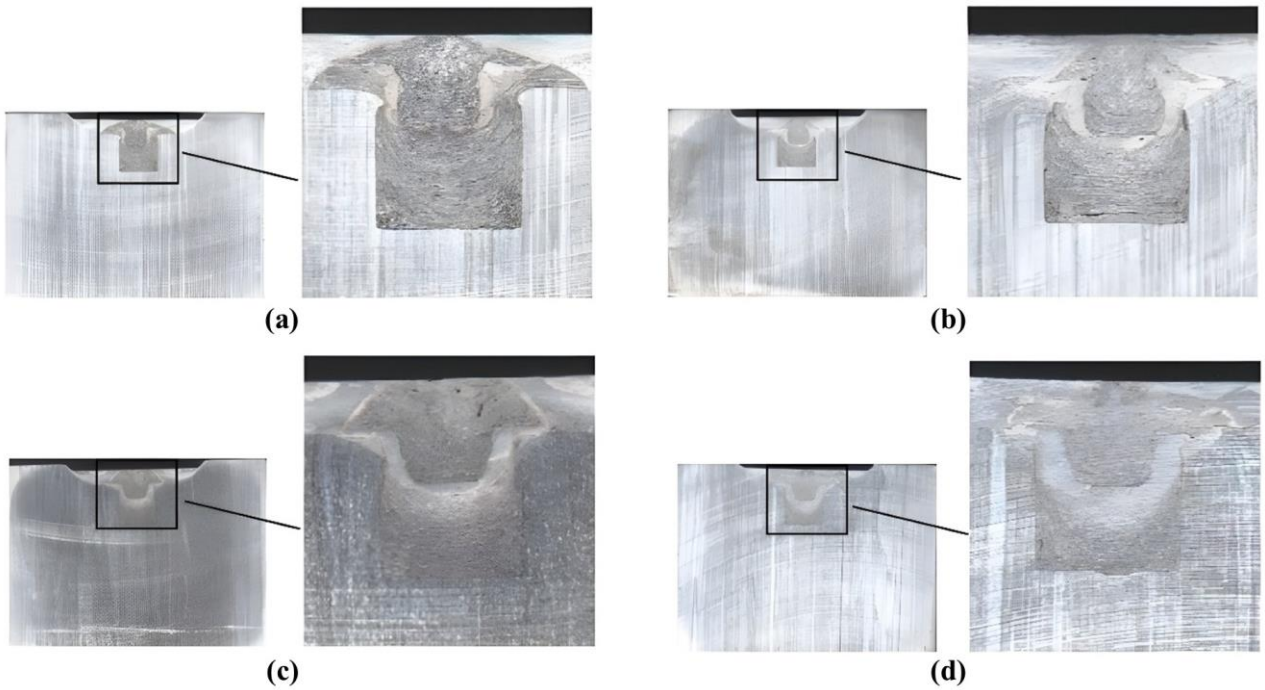

Fig. 3. Joint cross-section. (a) #1: 1250 rpm and 10 seconds, (b) #2: 1250 rpm and 20 seconds, (c) #3: 1600 rpm and 10 seconds, (d) #4: 1600 rpm and 20 seconds.

stirring were generated to properly consolidate the chips and bond them to the cavity wall. Consequently, incomplete consolidation occurred, manifested as significant porosity (dark regions and voids) within the cavity. The interfacial bonding with the parent material was also weak and discontinuous. In specimen #2, since the holding time has increased compared to specimen #1, the generated heat increases, which causes a continuous weld structure with less porosity than specimen #1. However, the quality is still not good, and some interfacial bonding issues persist due to the relatively low rotational speed. In specimen #3, increasing the rotational speed to 1600 rpm significantly improves the consolidation of the chips into a denser plug compared to specimens #1 and #2. The higher speed generated more frictional heat, making the material more plastic. However, the short 10-second holding time is insufficient for complete bonding at the bottom of the weld. A clear defect line is visible at the bottom interface, indicating poor material flow and weak bonding in that area. In specimen #4, both the tool rotational speed and holding time have increased compared to specimen #1, creating sufficient heat and providing proper energy input. This resulted in excellent consolidation of the chips into a solid, nearly-void-free plug and superior bonding at the interface between the plug and the parent material on all sides. The material flow appears smooth and continuous, indicating that a strong metallurgical connection has been formed.

Fig. 4 shows the microstructure of different regions of the weld cross-section in specimen #4. Four different regions can be identified in the cross-section of the welded specimen, including the stir zone (SZ), the thermos-mechanically affected zone (TMAZ), the heat-affected zone (HAZ), and the base metal (BM). The stir zone occurs around the tool pin. In this region, a high rate of mechanical work is performed, causing mechanical recrystallization and a high strain rate, which reduces the distances between materials and creates stronger cohesion. The thermo-mechanically affected zone is influenced by both heat and a high strain rate due to the vertical movement and rotation of the tool. In this region, material cohesion is less than in the stir zone. The shape of the plasticized material observed near the cavity wall indicates an upward flow. The heat-affected zone is located in a part of the BM where no strain rate is applied and is only affected by heat. In this area, the material retains similar properties to the BM. As shown in

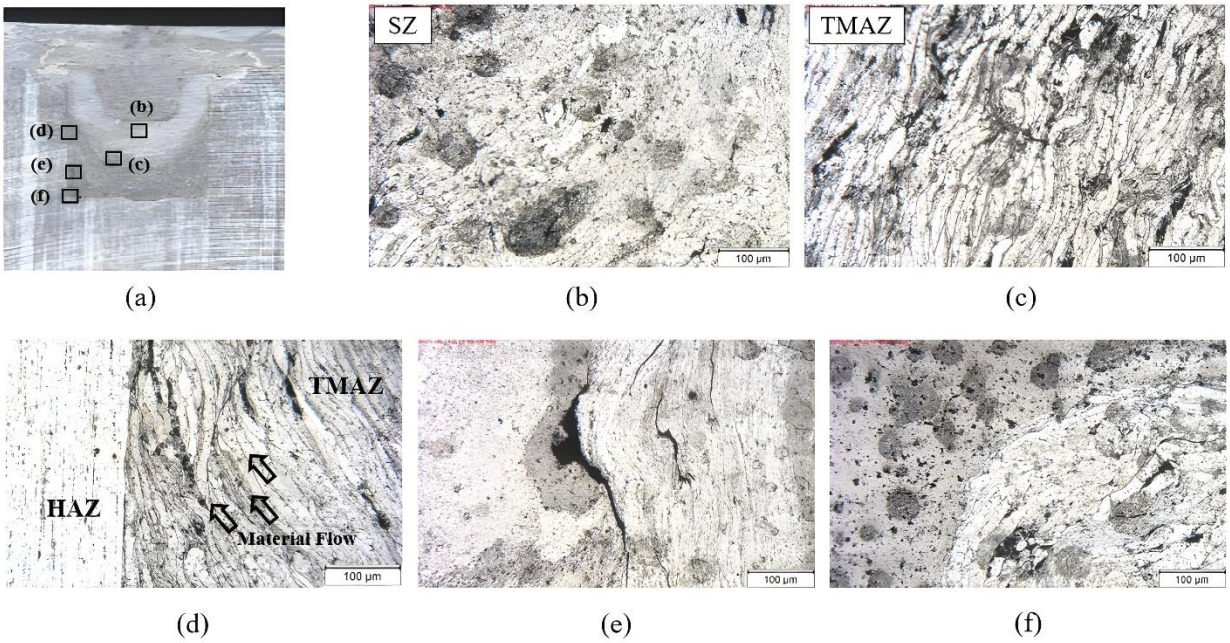

Fig. 4. Microstructure of different areas in the cross-section of the specimen #4 (1600 rpm in 20 s); (a) cross-section, (b) SZ, (c) TMAZ, (d) material flow pattern near the hole wall, (e) bottom corner of the hole, (f) filling defect and material flow.

Fig. 4(a), there is a bright, crescent-shaped area in the middle of all specimens. This crescent represents the connection area between the chips and the inner hole step. After preparing the specimens and filling the hole with chips, the first stage is performed with a pinless tool to prevent chips spillage. In the second stage, a conventional welding tool (pin tool) penetrates the hole until the tool pin enters the lower hole and the tool shoulder touches the lower hole step. To generate additional heat, after the tool shoulder touches the step, the tool is lowered another 1.5 mm until the shoulder is fully engaged with the lower step. This causes more heat and also removes the step. The material resulting from the partial solidification of the step and the chips combines and connects around the pin, flowing upward. This joint area becomes crescent-shaped and the microstructure images of this region show strong continuity due to sufficient heat input and also partial solidification of the base aluminum. The greater the thickness of this joint area, the greater the strength. This area in specimen #4 is thicker than in the other three specimens due to the higher heat generated and extends to the hole wall and is connected to it.

Fig. 4(b) shows the SZ with a very fine, uniform, and equiaxed grain structure. This results from dynamic recrystallization, where the intense heat and severe plastic deformation caused by the tool completely broke down the original grain structure and formed new, smaller grains. This fine-grained structure is highly desirable as it typically enhances the mechanical properties (strength and ductility) of the weld nugget. The dark, dispersed particles are likely fragments of intermetallic compounds from the base alloy, which have been broken up and distributed throughout the zone. In general, it can be asserted that according to the microstructure images from different regions, stir zone surrounding the pin experiences a reduction in tension and continuity as it approaches the bottom of the hole. This is attributed to the decreasing effects of heat and mechanical work on the chips as they get closer to the BM, combined with a reduction in temperature.

In Fig. 4(c) which shows the TMAZ, the material was heated and deformed, but not enough to cause full recrystallization. As a result, the original grains are severely elongated and bent upwards, clearly showing the flow of plasticized material as it was displaced by the rotating tool.

Fig. 4(d) clearly illustrates the interface between the undeformed HAZ and the highly deformed TMAZ. It shows excellent material flow along the hole wall, which

is critical for creating a strong bond. Fig. 4(e) shows that the material has successfully flowed into the bottom corner of the hole, demonstrating good consolidation in this hard-to-fill region.

The corner area of the bottom of the cavity is highly prone to porosity and pitting. This region experiences low heat and mechanical work because it is the furthest from the stir zone, which reduces mixing and makes it difficult for the kneaded materials to reach it. The most critical observation, derived from Fig. 4(f), is the presence of a filling defect characterized by a void formed due to incomplete fusion of the plasticized material. This type of defect forms when material flows around a point but lacks the final pressure or movement necessary to produce a solid-state weld in that spot. It could be caused by insufficient material flow reaching that precise area before the weld began to cool and solidify. Fig. 5 provides a powerful, direct comparison between a poor-quality weld (specimen #1) and a sound weld (specimen #4) in this spot, highlighting the critical role of process parameters. The low-energy weld shows gross porosity and a complete lack of bonding, while the high-energy weld shows excellent consolidation and bonding. There is a clear lack of bonding in Fig. 5(b), both between the individual chips and between the chip mass and the parent material (visible at the top of the micrograph). In contrast, the material in Fig. 5(c) is well-consolidated and dense. The severe plastic deformation has forged the individual chips into a coherent mass with clear, swirling flow patterns. A strong metallurgical bond has formed with the parent material at the interface.

MIP Cloud software was used to calculate the porosity percentage in the microstructure of the specimens within the stir zone (SZ), as shown in Fig. 6. According to the obtained results, it can be concluded that increasing the heat input leads to a decrease in porosity. The lowest porosity percentage in each specimen is observed in the stir zone. Furthermore, the farther the distance from the stir zone, the higher the porosity percentage becomes. Consequently, the bottom corner of the hole exhibits the highest porosity. By comparing porosity percentage among different specimens, it is observed that specimen #1 exhibits severe porosity. A significant portion of the stir zone consists of voids, indicating that this is not a proper weld but rather a loosely compacted mass of chips. In specimen #2, increasing the holding time noticeably reduced porosity compared to specimen #1; however, the porosity level remains unacceptably high for a sound weld. In specimen #3, increasing the rotational speed also reduces porosity significantly compared to specimen #1. The higher speed generated more heat and improved material flow, yet the short holding time was insufficient to eliminate all the voids. Finally, specimen #4 shows a drastic reduction in porosity, representing the highest quality weld among all specimens. The stir zone is dense and well-consolidated. In summary, both process parameters -tool rotational speed and holding time- directly influence the total heat and the degree of mechanical stirring. Higher rotational speed and longer holding time generate greater frictional heat, which softens the machining chips, making them more plastic and easier to forge together. The mechanical stirring action of the tool plays a key role in consolidating the softened chips. A more vigorous and prolonged stirring action, resulting from higher RPM and longer duration, is more effective in promoting material flow, filling voids, and expelling trapped air that would otherwise form pores.

Since the material undergoes high deformation and elevated temperatures during the friction stir welding process, microstructural changes such as sediment coarsening and recrystallization can be expected in the joint areas. In the case of heat-treatable aluminum alloys, due to the production of high working temperatures during the process in the SZ and a small amount in the TMAZ, some of the sedimentary phases are dissolved and as a result, some softening is expected in the weld area. Rockwell hardness tests with a load of 60 kgf were performed to determine the hardness values at different areas across the weld cross-sections of all welded specimens, as shown in Fig. 7. It can be seen that the lowest hardness value in each specimen corresponds to the bottom corner of the hole (point 5). The results also

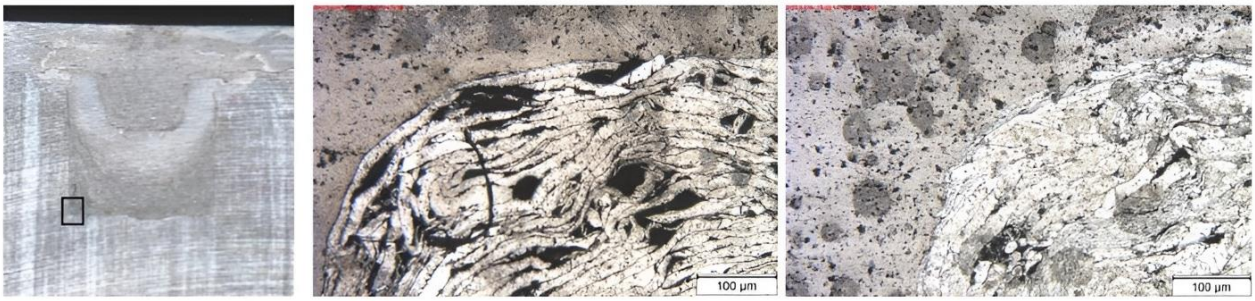

Fig. 5. a) Compared area in cross-section of two specimens. b) #1: 1250 rpm in 10 s, c) #4: 1600 rpm in 20 s.

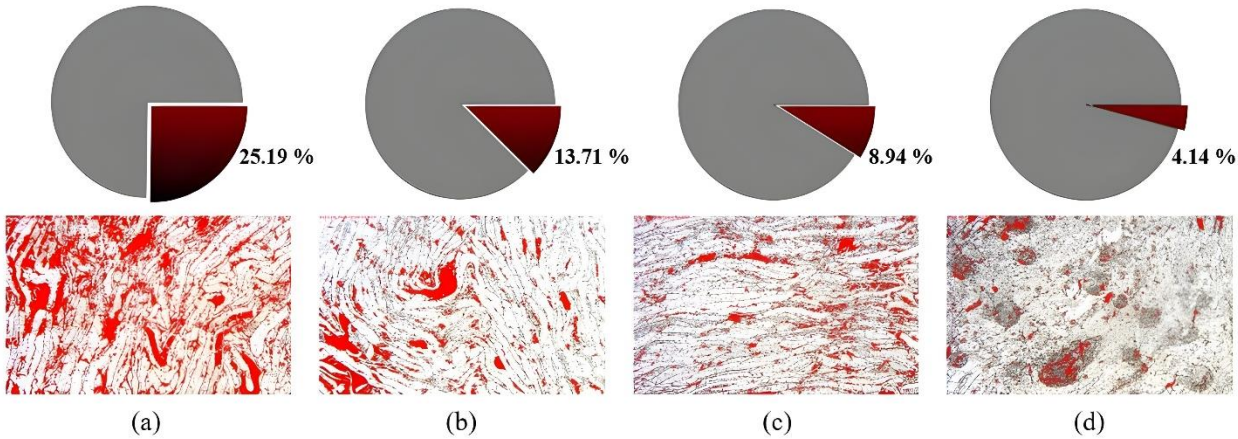

Fig. 6. Porosity percentages of the stir zones in specimens. (a) #1: 1250 rpm in 10 s, (b) #2: 1250 rpm in 20 s, (c) #3: 1600 rpm in 10 s, (d) #4: 1600 rpm in 20 s.

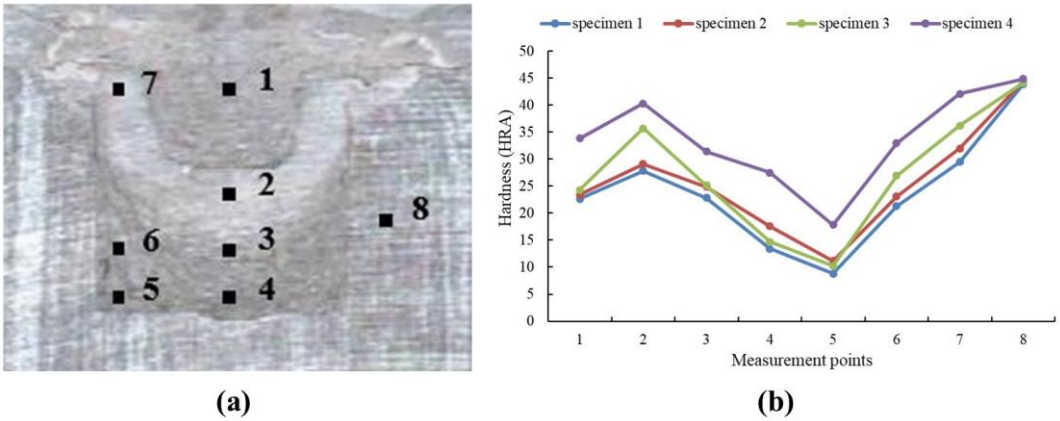

Fig. 7. (a) Hardness test points in the cross-section of the specimens, (b) hardness values in different welding areas (measured points).

show that weld hardness increases directly with higher energy input, with Specimen #4 (1600 rpm, 20s) exhibiting the highest hardness and best robustness. The primary reason for this improvement is the enhanced consolidation of the weld and the significant reduction in porosity.

All specimens display a similar "W-shaped" hardness profile, which is typical for friction stir welds in heat-treatable aluminum alloys. The lowest hardness occurs in the heat-affected regions on the weld edge (point 5), while the highest values are observed in the unaffected base material (point 8). The central stir zone (points 1-4) shows hardness values lower than the base material but significantly higher than those of the

softened heat-affected zones. Moreover, the hardness values are in good agreement with the microstructure images and porosity measurements. For example, Specimen #4, which shows a more continuous microstructure and a lower porosity percentage, exhibits higher hardness compared to the other specimens. To observe the effect of tool rotational speed on hardness in different weld areas, specimens with the same holding time were compared. It is observed that the greatest hardness increase resulting from higher tool rotational speed occurred in the SZ and adjacent areas. As the distance from the SZ increased, the rate of hardness improvement diminished. For instance, by comparing specimens #1 and #3, both welded with a 10 s holding time but at different rotational speeds of 1250 and 1600 rpm, the SZ hardness increased significantly from 27.8 HRA to 35.7 HRA, while at the bottom of the hole, the increase was minor from 8.8 HRA to 10.2 HRA. With increasing the holding time in specimens obtained from welding with the same rotational speed, it was observed that the greatest increase in hardness is related to the areas further away from the SZ and TMAZ. Extending the holding time enhanced material flow to the farther regions, reducing porosity and improving cohesion. As a result, the outer regions experienced a greater hardness increase. For example, by comparing specimens #3 and #4 (both at 1600 rpm but with holding times of 10 s and 20 s, respectively), it was observed that while hardness increased in all areas, the percentage increase was higher at the bottom of the hole areas farther from the SZ. In the SZ, hardness increased from 35.7 HRA to 40.3 HRA, whereas at the bottom of the hole, it rose from 10.2 HRA to 17.8 HRA. In all specimens, the SZ (the bright area) shows the highest hardness compared to other regions of the same specimen and also exhibits values closest to those of the BM. This behavior is attributed to the intense heat and friction generated by the tool pin and the shoulder, as well as the mixing of chips with the plasticized material from the lower hole step caused by the tool shoulder.

The friction stir chip welding (FSCW) method represents a convergence of solid-state repair and recycling principles, and its performance can be benchmarked against both domains. The observed "W-shaped" hardness profile (Fig. 7) is consistent with friction stir processing of aluminum alloys [7, 13]. However, the recovered stir zone (SZ) hardness (40.3 HRA for specimen #4) signifies an improvement over typical FSW softening. This enhancement, attributable to the fine-grained structure formed by the direct consolidation of chips, positions FSCW favorably against analogous repair methods such as multilayer friction stir plug welding [13].

When evaluated against chip-recycling techniques, FSCW's ability to achieve low porosity (Fig. 6) demonstrates its efficacy in meeting the fundamental consolidation criterion of attaining near-full density, a primary objective in friction stir consolidation [16]. However, FSCW extends this capability by simultaneously creating a metallurgical bond with the base plate, a feature not reported in standalone consolidation studies [16, 23]. The systematic microhardness mapping (Fig. 7) provides a critical advancement over prior chip-refilling investigations [23], as it quantitatively demonstrates that the recycled material in the SZ can achieve mechanical properties comparable to those of the base metal.

Furthermore, FSCW addresses common process-specific challenges, such as the mitigation of bottom-corner filling defects (Fig. 4f), through optimized parameters that enhance material flow, a known issue in blind-hole refilling [5, 11]. The overarching novelty of the process lies in its integrated approach, which unites recycling and repair in a single operation, thereby eliminating the need for intermediate billet production [14, 16]. The validation of a pinless pre-heating stage, a strategy corroborated by an independent study [13], underscores a universal requirement for defect-free outcomes in such complex solid-state operations.

4. Conclusions

In the present study, a method for removing and repairing deep cracks using waste chips, based on the friction stir welding principle, was introduced. This process, termed friction stir chip welding (FSCW), was investigated with respect to its key parameters -tool

rotational speed and holding time- and their effects on joint quality, microstructure, and hardness across different weld regions. The main findings can be summarized as follows:

- FSCW is an effective method for repairing cracks and holes in thick aluminum plates.
- The most critical parameter for creating a proper joint and material flow is the input heat, which is affected by the tool rotational speed and holding time. An increase in either parameter enhances heat generation.
- Based on the microstructure observations, as the distance from the stir zone (SZ) increases and approaches the base metal (BM), the structural cohesion and continuity decrease while porosity increases. This is attributed to a reduction in temperature.
- The highest porosity (25.19%) was observed at the bottom corner of the cavity under the lowest energy condition (tool rotational speed of 1250 rpm and holding time of 10 s)
- Both the tool rotational speed and holding time significantly affect the hardness distribution across the weld. For specimens welded at the same rotational speed, the greatest increase occurs in regions farther from the SZ. Conversely, for specimens welded with the same holding time, the most notable hardness increase occurs within and near the SZ areas.

For future research, it is recommended to explore the effects of chip volume and pressing pressure during the first stage. Although not considered as variables in this study, it is crucial to use the correct volume of machining chips. Too little chip volume will result in void formation, while excessive filling may create excessive flash and potentially affect clamping pressure.

Authors' Contributions

A. Bazrafshan Tanha: Conceptualization, Methodology, Writing- Original Draft, Visualization

S. M. H. Seyedkashi: Project administration, Supervision, Writing- Review & Editing

M. Sajed: Methodology, Writing- Review & Editing

H. Rastegari: Resources, Validation

Conflict of interest

The authors declare no competing interests.

Data availability

The datasets generated during and/or analyzed during the current study are available from the corresponding author upon reasonable request.

Funding

This research did not receive any specific grant from funding agencies in the public, commercial, or not-for-profit sectors.

5. References

[1] Heidarzadeh, A., Barenji, R. V., Esmaily, M., & Ilkhichi, A. R. (2015). Tensile properties of friction stir welds of AA 7020 aluminum alloy. *Transactions of the Indian Institute of Metals*, *68*, 757–767. https://doi.org/10.1007/s12666-014-0508-2

[2] Wen, Q., Li, W., Wang, W., Wang, F., Gao, Y., & Patel, V. (2019). Experimental and numerical investigations of bonding interface behavior in stationary shoulder friction stir lap welding. *Journal of Materials Science & Technology*, *35*(1), 192–200. https://doi.org/10.1016/j.jmst.2018.09.028

[3] Liu, H., Zhao, Y., Su, X., Yu, L., & Hou, J. (2013). Microstructural characteristics and mechanical properties of friction stir spot welded 2A12-T4 aluminum alloy. *Advances in Materials Science and Engineering*, 2013, 719306. https://doi.org/10.1155/2013/719306

[4] Li, G., Zhou, L., Luo, L., Wu, X., & Guo, N. (2019). Microstructural evolution and mechanical properties of refill friction stir spot welded alclad 2A12-T4 aluminum alloy. *Journal of Materials Research and Technology*, *8*(5), 4115–4129. https://doi.org/10.1016/j.jmrt.2019.07.021

[5] Jo, D. S., Kim, J. H., & Kim, B. M. (2019). Feasibility study on application of hot forming quenching to patchwork blanks using two-stage refilled friction stir spot welding. *Journal of Manufacturing Processes*, *41*, 66–73. https://doi.org/10.1016/j.jmapro.2019.03.012

[6] Sharma, Y., Singh, K. J., & Vasudev, H. (2022). Experimental studies on friction stir welding of aluminium alloys. *Materials Today: Proceedings*, *50*, 2387–2391. https://doi.org/10.1016/j.matpr.2021.10.254

[7] Malopheyev, S., Vysotskiy, I., Kulitskiy, V., Mironov, S., & Kaibyshev, R. (2016). Optimization of processing-microstructure-properties relationship in friction-stir welded 6061-T6 aluminum alloy. *Materials Science and*

Engineering: A, *662*, 136–143. https://doi.org/10.1016/j.msea.2016.03.063

[8] Ahmed, M. M. Z., El-Sayed Seleman, M. M., Ahmed, E., Reyad, H. A., Touileb, K., & Albaijan, I. (2022). Friction stir spot welding of different thickness sheets of aluminum alloy AA6082-T6. *Materials*, *15*(9), 2971. https://doi.org/10.3390/ma15092971

[9] Fereiduni, E., Movahedi, M., & Kokabi, A. H. (2015). Aluminum/steel joints made by an alternative friction stir spot welding process. *Journal of Materials Processing Technology*, *224*, 1–10. https://doi.org/10.1016/j.jmatprotec.2015.04.028

[10] Yuan, T., Kang, S., Jiang, X., & Zhao, P. (2023). Exit-hole repairing in 7475 aluminium alloy welded joints based on refill friction stir processing. *Science and Technology of Welding and Joining*, *28*(8), 819–828. https://doi.org/10.1080/13621718.2023.2235791

[11] Li, M., Zhang, C., Wang, D., Zhou, L., Wellmann, D., & Tian, Y. (2019). Friction stir spot welding of aluminum and copper: a review. *Materials*, *13*(1), 156. https://doi.org/10.3390/ma13010156

[12] Sajed, M. (2016). Parametric study of two-stage refilled friction stir spot welding. *Journal of Manufacturing Processes*, *24*, 307–317. https://doi.org/10.1016/j.jmapro.2016.09.011

[13] Sajed, M., & Seyedkashi, S. H. (2020). Multilayer friction stir plug welding: A novel solid-state method to repair cracks and voids in thick aluminum plates. *CIRP Journal of Manufacturing Science and Technology*, *31*, 467–477. https://doi.org/10.1016/j.cirpj.2020.07.009

[14] Shigematsu, I., Suzuki, K., Imai, T., Kwon, Y. J., & Saito, N. (2005). Friction stir welding of recycled A6061 aluminum plates fabricated by hot-extrusion of machined chips. *Journal of Materials Science*, *40*(11), 2971–2974. https://doi.org/10.1007/s10853-005-2390-0

[15] Haase, M., & Tekkaya, A. E. (2014). Recycling of aluminum chips by hot extrusion with subsequent cold extrusion. *Procedia Engineering*, *81*, 652–657. https://doi.org/10.1016/j.proeng.2014.10.055

[16] Li, X., Baffari, D., & Reynolds, A. P. (2018). Friction stir consolidation of aluminum machining chips. *The International Journal of Advanced Manufacturing Technology*, *94*, 2031–2042. https://doi.org/10.1007/s00170-017-1016-4

[17] El-Mehtedi, M., Forcellese, A., Mancia, T., Simoncini, M., & Spigarelli, S. (2019). A new sustainable direct solid state recycling of AA1090 aluminum alloy chips by means of friction stir back extrusion process. *Procedia CIRP*, *79*, 638–643. https://doi.org/10.1016/j.procir.2019.02.062

[18] Abbas, A. T., Taha, M. A., Ragab, A. E., El-Danaf, E. A., & Abd El Aal, M. I. (2017). Effect of equal channel angular pressing on the surface roughness of solid state recycled aluminum alloy 6061 chips. *Advances in Materials Science and Engineering*, 2017, 5131403. https://doi.org/10.1155/2017/5131403

[19] Yavari Nouri, M., Seyedkashi, S. M. H., & Sajed, M. (2021). Experimental investigation on process parameters of dissimilar double-layered wire produced by modified friction stir extrusion process. *International Journal of Advanced Design and Manufacturing Technology*, *14*(3), 1–7. https://doi.org/10.30495/admt.2021.1911339.1220

[20] Laurent-Brocq, M., et al. (2023). Solid state recycling of aluminium chips: Multi-technique characterization and analysis of oxidation. *Materialia*, *31*, 101864. https://doi.org/10.1016/j.mtla.2023.101864

[21] Buffa, G., Campanella, D., Adnan, M., La Commare, U., Ingarao, G., & Fratini, L. (2024). Improving the industrial efficiency of recycling aluminum alloy chips using friction stir extrusion: thin wires production process. *International Journal of Precision Engineering and Manufacturing - Green Technology*, *11*, 1133–1146. https://doi.org/10.1007/s40684-023-00573-w

[22] Carta, M., Ben Khalifa, N., Buonadonna, P., El Mohtadi, R., Bertolino, F., & El Mehtedi, M. (2024). Innovative solid-state recycling of aluminum alloy AA6063 chips through direct hot rolling process. *Metals*, *14*(12), 1442. https://doi.org/10.3390/met14121442

[23] Bhardwaj, N., Ganesh Narayanan, R., & Dixit, U. S. (2020). Refilling of pinhole in friction stir spot welding using waste chips. In M. Shunmugam & M. Kanthababu (Eds.), *Advances in Additive Manufacturing and Joining* (pp. 417–426). Springer. https://doi.org/10.1007/978-981-32-9433-2_34

[24] Wan, B., Chen, W., Lu, T., Liu, F., Jiang, Z., & Mao, M. (2017). Review of solid state recycling of aluminum chips. Resources, *Conservation & Recycling*, *125*, 37–47. https://doi.org/10.1016/j.resconrec.2017.06.004

[25] Altharan, Y. M., Shamsudin, S., Al-Alimi, S., Saif, Y., & Zhou, W. (2024). A review on solid-state recycling of aluminum machining chips and their morphology effect on recycled part quality. *Heliyon, 10*, e34433. https://doi.org/10.1016/j.heliyon.2024.e34433

[26] Murray, J. W., et al. (2024). A review of principles and options for the re-use of machining chips by solid, semi-solid or melt-based processing. *Journal of Materials Processing Technology*, *331*, 118514. https://doi.org/10.1016/j.jmatprotec.2024.118514

[27] Han, J., Paidar, M., Vignesh, R. V., Mehta, K. P., Heidarzadeh, A., & Ojo, O. O. (2020). Effect of shoulder features during friction spot extrusion welding of 2024-T3 to 6061-T6 aluminium alloys. *Archives of Civil and Mechanical Engineering*, *20*(3), 84. https://doi.org/10.1007/s43452-020-00086-2

[28] Heidarzadeh, A., Javidani, M., Mofarrehi, M., Farzaneh, A., & Chen, X. G. (2021). Submerged dissimilar friction stir welding of AA6061 and AA7075 aluminum alloys: Microstructure characterization and mechanical property. *Metals*, *11*(10), 1592. https://doi.org/10.3390/met11101592

[29] Panda, B., Garg, A., Jian, Z., Heidarzadeh, A., & Gao, L. (2016). Characterization of the tensile properties of friction stir welded aluminum alloy joints based on axial force, traverse speed, and rotational speed. *Frontiers of Mechanical Engineering*, *11*(3), 289-298. https://doi.org/10.1007/s11465-016-0393-y

[30] Çam, G., Javaheri, V., & Heidarzadeh, A. (2023). Advances in FSW and FSSW of dissimilar Al-alloy plates. *Journal of Adhesion Science and Technology*, *37*(2), 162-194. https://doi.org/10.1080/01694243.2022.2028073

[31] Baffari, D., Reynolds, A. P., Masnata, A., Fratini, L., & Ingarao, G. (2019). Friction stir extrusion to recycle aluminum alloys scraps: Energy efficiency characterization. *Journal of Manufacturing Processes*, 43, 63-69. https://doi.org/10.1016/j.jmapro.2019.03.049

[32] Iwaszko, J., & Sajed, M. (2021). Technological aspects of producing surface composites by friction stir processing—A review. *Journal of Composites Science*, *5*(12), 323. https://doi.org/10.3390/jcs5120323

[33] Akbari, M., Asadi, P., Behnagh, R. A., Bedir, F., Choupani, N., & Sadowski, T. (2025). Process parameters and tool design in friction stir extrusion: A sustainable recycling technique. *Engineering Reports*, *7*(1), e13060. https://doi.org/10.1002/eng2.13060